HHS Public Access

Author manuscript

Kidney Int. Author manuscript; available in PMC 2018 September 01.

Published in final edited form as:

Kidney Int. 2017 September ; 92(3): 657–668. doi:10.1016/j.kint.2017.02.017.

B-type natriuretic peptide overexpression ameliorates hepatorenal fibrocystic disease in a rat model of polycystic kidney disease

Sara J. Holditch, Ph.D[1], **Claire A. Schreiber, B.S**[1], **Peter C. Harris, Ph.D**[2], **Nicholas F. LaRusso, M.D**[3], **Marina Ramirez-Alvarado, Ph.D**[4], **Alessandro Cataliotti, M.D, Ph.D**[5], **Vicente E. Torres, M.D, Ph.D**[2], and **Yasuhiro Ikeda, D.V.M, Ph.D**[1,*]

[1]Department of Molecular Medicine, Mayo Clinic, Rochester, MN, 55905

[2]Division of Nephrology and Hypertension, Mayo Clinic Translational Polycystic Kidney Disease Center, Mayo Clinic, Rochester, MN, 55905

[3]Division of Gastroenterology, Mayo Clinic, Rochester, MN, 55905

[4]Department of Biochemistry and Molecular Biology, Mayo Clinic, Rochester, MN, 55905

[5]Institute for Experimental Medical Research, Oslo University Hospital, University of Oslo, Oslo, Norway

Abstract

Polycystic kidney disease (PKD) involves progressive hepatorenal cyst expansion and fibrosis, frequently leading to end-stage renal disease. Increased vasopressin and cAMP signaling, dysregulated calcium homeostasis, and hypertension play major roles in PKD progression. The guanylyl cyclase A agonist, B-type natriuretic peptide (BNP), stimulates cGMP and shows anti-fibrotic, anti-hypertensive, and vasopressin-suppressive effects, potentially counteracting PKD pathogenesis. Here, we assessed the impacts of guanylyl cyclase A activation on PKD progression in a rat model of PKD. Sustained BNP production significantly reduced kidney weight, renal cystic indexes and fibrosis, in concert with suppressed hepatic cystogenesis *in vivo*. *In vitro*, BNP decreased cystic epithelial cell proliferation, suppressed fibrotic gene expression, and increased intracellular calcium. Together, our data demonstrate multifaceted effects of sustained activation of

[*]**Corresponding author**: Yasuhiro Ikeda, Department of Molecular Medicine, Mayo Clinic College of Medicine, 200 First Street SW, Rochester, MN 55905, Tel: 507-538-1252; Fax: 507-266-2122; ikeda.yasuhiro@mayo.edu.

CONTRIBUTIONS

SJH – designed research studies, conducted experiments, analyzed data, wrote and edited the manuscript
CAS – conducted experiments, analyzed data, edited the manuscript
AC, PCH, NFLR - edited the manuscript
MRA, VET - designed research studies, offered insight in the analysis of data, edited the manuscript
YI - designed research studies, offered insight in the analysis of data, wrote and edited the manuscript

DISCLOSURE

None.

guanylyl cyclase A on polycystic kidney and liver disease. Thus, targeting the guanylyl cyclase A-cGMP axis may provide a novel therapeutic strategy for hepatorenal fibrocystic diseases.

Keywords

ARPKD; ADPKD; Congenital hepatic fibrosis; gene therapy; adeno-associated virus

INTRODUCTION

Autosomal dominant polycystic kidney disease (ADPKD) is characterized by focal development and expansion of cysts, frequently leading to end-stage renal disease (ESRD).[1, 2] Autosomal recessive PKD (ARPKD) is characterized by diffuse fusiform dilatation of the collecting ducts causing massive renal enlargement at birth, followed by interstitial fibrosis, early onset ESRD,[3] and congenital hepatic fibrosis. Arginine vasopressin (AVP), epithelial proliferation, and hypertension are major contributors in PKD progression. At a molecular level, causative-PKD proteins are involved in calcium (Ca^{2+}) signaling and alterations in intracellular Ca^{2+} $[Ca^{2+}]_i$ homeostasis may play a role in the upregulation of cyclic AMP (cAMP) and protein kinase A (PKA) signaling observed in cystic tissues.[4, 5]

B-type natriuretic peptide (BNP) binds guanylyl cyclase A (GC-A/NPRA) to stimulate the cyclic GMP (cGMP) pathway. Through activation of cGMP-dependent kinases (PKGs) and modulation of $[Ca^{2+}]_i$, BNP elicits vasodilating, natriuretic, and anti-hypertrophic effects *in vivo*.[6] BNP also inhibits fibroblast proliferation and down-regulates fibrosis-associated genes such as *Tgfβ*, *Col1a1*, and *Fn1*, and suppresses AVP release.[7] We showed BNP knockout $Nppb^{-/-}$ rats developed interstitial fibrosis and glomerulosclerosis prior to the development of hypertension, suggesting an intrinsic renoprotective role, separate from BNPs' anti-hypertensive propensity.[8] Further, BNP-transgenic mice are resistant to glomerular injury upon renal ablation, glomerulonephritis, and chemically induced diabetic nephropathy.[9, 10]

Since destruction of renal parenchyma is principally responsible for declining kidney function, early interventions aimed at preventing cyst expansion are critical for PKD therapy. BNPs' properties, and the potential of the GC-A/cGMP pathway, promise multiple points of intervening PKD pathobiology. However, the role of cGMP in PKD is poorly understood. Increased levels of cGMP have been observed in the kidneys of PKD animals,[11] however 8-Br-cGMP does not stimulate human PKD cyst-derived cell proliferation.[12] In this study, we assessed BNP overexpression *in vitro*, and *in vivo* on the development of hepatorenal cysts and fibrosis in the PCK rat, an orthologous rat model of ARPKD, with human ADPKD-like hepatorenal pathology.[13, 14]

RESULTS

Adeno-associated viral (AAV) vector-mediated systemic BNP overexpression stimulates cGMP, suppresses circulating AVP, and improves cardiac function

Due to a short *in vivo* half-life, long-term BNP therapy has been challenging. To address this, we used AAV serotype 9 (AAV9) vectors, carrying CMV-driven codon-optimized

proBNP cDNA.[15] BNP transgene expression was determined in a rat model of PKD (PCK rats) treated with 10^{13} vg/kg AAV9-BNP. Three months post injection, RT-PCR detected significantly increased transgene BNP transcripts in the heart, liver, and kidney (Fig. 1a). In contrast, endogenous BNP transcripts were comparable between AAV9-BNP and control littermates (Fig. 1b). There was no significant increase in circulating BNP levels between low-dose AAV9-BNP (10^{13} vg/kg) and littermate controls, while High-Dose (HD) AAV9-BNP (10^{14} vg/kg) demonstrated significantly elevated circulating BNP (Fig. 1c). Unenhanced serum levels of BNP with low-dose AAV9-BNP may be due to rapid enzymatic degradation (e.g. by neprilysin) and/or clearance through NPR-C.[16] Nevertheless, excreted cGMP was elevated (Fig. 1d), indicating *in vivo* cGMP stimulation by low-dose AAV9-BNP. Similarly, blood from terminal cardiac puncture demonstrated reduced CT-proAVP, an indicator of AVP levels[17], with low-dose AAV9-BNP (Fig. 1e). At 3 months of age, PCK rats remained normotensive (Fig. 1f). Although effects were modest, left ventricular ejection fraction and percent fractional shortening were significantly higher with treatment (Fig. 1g), suggesting improved cardiac function upon BNP treatment.

BNP renal effects in PCK rats

Three months after low-dose AAV9-BNP administration treated PCK displayed reduced 24-hour urine excretion. Although total urine metabolites per 24-hour collection were relatively uninfluenced, sodium and potassium concentrations were significantly increased with AAV9-BNP (Fig. 2a). Further, total urinary protein was reduced (Fig. 2a), and plasma albumin levels were significantly increased with treatment (Sup. Fig. S1). Creatinine clearance was significantly higher with AAV9-BNP, comparable to Sprague Dawley (SD), non-PKD controls (Fig. 2b). Together, this suggests that BNP treatment increases urine concentrating capacity and glomerular filtration rate. At sacrifice, total kidney weight per body weight (TKW/BW) was reduced with AAV9-BNP compared to PCK controls (12.6 ± 1.7 vs 14.5 ± 2.0 mg/g), without a difference in body weight between treatment (Fig. 2c). Histology revealed renal cysts in PCK controls, and a reduced (40%) cystic index with AAV9-BNP (Fig. 2d, 2e). Additionally, fewer injured glomeruli were observed by H&E staining with BNP treatment (Fig. 2f). Reduced urinary excretions of kidney injury molecule-1 (Fig. 2g) and neutrophil gelatinase-associated lipocalin (262.5±6.6 vs. 293.2±11.6 ng/ml in controls) were observed, suggesting reduced renal injury with AAV9-BNP. AAV9-BNP treated animals exhibited reduced fibroblast growth factor 2 (Fgf2), and inflammation marker, Desmin, expression as indicated by immunofluorescence (IF) staining (Fig. 2h, 2i), and trends in reduced renal fibrosis, assessed by Trichrome staining (Fig. 2j, 2k). RT-PCR of profibrotic gene expression in renal tissues were significantly reduced collagen type 1 (*Col1a1*), fibronectin (*Fn1*), and *Tgfβ* transcripts in treated PCK (Fig. 2l). Despite renoprotective effects with BNP treatment, total renal cAMP levels were increased in treated PCK (Fig. 2m).

To better define the pathways affected by AAV9-BNP treatment, we performed genome-wide transcriptome analysis in renal RNA of treated and control PCK rats. Transcriptome analysis revealed suppression of collagen genes, *Col3a1, Col5a2, Col6a3, Col6a1 and Col8a2*, with BNP treatment (Sup. Fig. S2). Intriguingly, bioinformatic analysis identified the top 10 differentially expressed signaling pathways as PTEN, aldosterone, PDGF, ErbB2-

ErbB3, IL-8, PI3K/AKT, Her2/ErbB2, and NFAT (Sup. Fig. S2, S3, S4, S5 and S6), pathways routinely implicated in PKD pathogenesis.[18, 19] Wnt signaling and negative regulators for calcineurin/NFAT were also identified as influenced pathways with BNP treatment, whereas no significant changes were observed in natriuretic peptide system genes (Sup. Fig. S2).

Reduced hepatic cystic lesions, fibrosis, and profibrotic gene expression in PCK rats with sustained BNP overexpression

In addition to renal cystogenesis and fibrosis, PCK rats exhibit congenital liver fibrosis, characterized by progressive fibropolycystic liver disease. We therefore characterized the influence of BNP overexpression in the liver of PCK rats. Pathological analysis of liver tissue demonstrated reduced hepatic remodeling (Fig. 3a, upper panels) and cystic indices (Fig. 3b) in AAV9-BNP treated PCK. When fibrotic regions were visualized by picrosirius red (PSR) staining, we found a trend of reduced connective tissue areas (Fig. 3a, lower panels and Fig. 3c). However, collagen content, quantified by hydroxyproline, detected no notable difference between groups (Fig. 3d). IF staining demonstrated reduced Desmin-positive hepatic stellate cells, reduced fibrosis regulator galectin-3, and CK7-positive cholangiocytes in BNP treated PCK hepatic sections (Fig. 3e, 3f). Desmin-positive cells were predominantly negative for αSMA staining in both groups (Fig. 3e). RT-PCR showed reduced transcripts of *Fn1, Tgfβ*, and *Desmin* with BNP treatment, although *Col1a1* and *Timp1* expression was not affected (Fig. 3g). This suggests that BNP provides liver protection through reduced hepatic cyst expansion, restrained expansion of Desmin-positive stellate cells and CK7-positive cholangiocytes, and suppression of a subset of profibrotic genes, such as *Tgfβ*.

Influence of a higher dose AAV9-BNP in PCK rats

To further understand tolerability of the AAV9-BNP vector, we administered a 10-fold higher dose (HD AAV9-BNP, 10^{14} vg/kg), resulting in 40-fold increased circulating levels of BNP (Fig. 1c). Supraphysiological BNP did not induce hypotension (Sup. Fig. S7a) or notable differences in blood chemistry parameters (Sup. Fig. S7b). Four months after AAV administration, rats were sacrificed. Compared to 3 month-old PCK controls (Fig. 2c, d, e), 4 month-old PCK rats exhibited advanced cystogenesis and increased TKW/BW (Sup. Fig. S8a, b, c). HD AAV9-BNP resulted in trends of better preserved renal architecture, reduced TKW/BW, and smaller cystic indices (Sup. Fig. S8a, b, c and d), though statistical significance was not achieved. We also found trends of reduced hepatic remodeling and cystic indices in HD AAV9-BNP rats (Sup Fig. S8e, 8f, 8g, Sup. Fig. S9). At this time point, control PCK rats showed αSMA-positive cells in the liver, a population which appeared less prominent in HD AAV9-BNP-treatment (Sup. Fig. S8h). Lastly HD AAV9-BNP treatment seemed to have increased mortality within 2 months of vector administration (Sup. Fig. S8i); however, no statistical significance was found in survival between groups.

BNP treatment reduces proliferation and increases $[Ca^{2+}]_i$ in epithelial cells

To better characterize direct cellular effects of BNP, we treated cholangiocytes from PCK and SD with BNP. Non- and cystic cholangiocytes treated with BNP for 72 hours exhibited significantly reduced proliferation compared to vehicle (Fig. 4a, left panel). Levels of

$[Ca^{2+}]_i$ assessed with Fura-2AM were increased with BNP in cystic cholangiocytes (Fig. 4a, right panel). BNP- or GFP-lentiviral transduction of ADPKD, ARPKD, and normal human renal epithelial (HRE) cells were then assayed to determine effects on proliferation or $[Ca^{2+}]_I$. BNP transduced cell lines responded with significantly reduced proliferation (Fig. 4b). Reduced HRE proliferation was associated with reduced levels of phosphorylated ERK, i.e. ERK activation, as demonstrated by reduced protein levels (Fig. 4c), and PKD HRE cells exhibited increased levels of $[Ca^{2+}]_i$ with BNP (Fig. 4d). Media supplemented with Ca^{2+} showed no notable influence on $[Ca^{2+}]_i$, suggesting that BNP-mediated increases were primarily due to a release of $[Ca^{2+}]_i$ stores. Since the endoplasmic reticulum (ER) is the largest store of $[Ca^{2+}]_i$ we assessed effects of two ER Ca^{2+} channel inhibitors on our transduced cell lines; a ryanodine receptor (RyR) inhibitor, JTV 519 fumarate, and an inhibitor of inositol triphosphate receptor (IP_3R), 2-aminoethoxydiphenyl borate (2-APB). Diminished $[Ca^{2+}]_i$ was observed in the presence of 2-APB, but not JTV 519 fumarate, suggesting that BNP increases $[Ca^{2+}]_i$ partly through IP_3R in cystic epithelial cells (Fig. 4e). Lastly, BNP overexpression in normal and cystic HRE cells significantly suppressed *COL1A1* and *TGFβ* transcripts relative to controls (Sup. Fig. S10).

DISCUSSION

Mechanisms of BNP therapy on PKD progression

BNP-transgenic mice are resistant to various experimental renal injuries with notable suppression of renal *Tgfβ* and *pERK*.[9, 10] PKD progression is known to be influenced by genetic mutations, genetic background, and hypertension.[20] BNP suppressed AVP release, demonstrated by reduced serum CT-proAVP levels. In accordance with potent anti-fibrotic effects of BNP,[21–24] we observed a trend of reduced fibrosis and significant suppression of profibrotic genes, including Tgfβ. Of note, Tgfβ signaling plays in cyst progression and fibrogenesis of both ADPKD murine models and ADPKD patients,[25, 26] while the inhibition of the activin/*Tgfβ* signaling pathway retards PKD progression.[27] BNP treatment also reduced glomerular injury and expression of inflammation marker Desmin in PCK rats. Gene expression profiling indicated that BNP treatment altered key PKD pathogenesis-associated pathways, such as PTEN, Aldosterone, PDGF, ErbB2/3, Her2, PI3K and calcineurin/NFAT. Additionally, *in vitro* BNP supplementation demonstrated a direct effect on epithelial cells, reduced proliferation, suppressed ERK activation, and increased $[Ca^{2+}]_i$. Thus, observed renal protective effects in BNP-treated PCK rats are likely due to multifaceted effects induced by BNP directly or indirectly.

It is known that cAMP inhibits proliferation of noncystic cells, while enhancing proliferation in cyst derived epithelial cells in a Src, Ras, B-Raf/ERK and mTOR dependent manner.[12, 28] This proliferative response has been linked to reduced $[Ca^{2+}]_i$, as illustrated by Ca^{2+} channel blockers inducing a proliferative response to cAMP in normal human kidney or murine collecting duct cells, whereas Ca^{2+} channel activators or Ca^{2+} ionophores restores a normal antimitogenic response to cAMP in ADPKD or ARPKD cyst-derived cells.[28, 29] Unexpectedly, BNP treatment did not reduce the total cAMP levels in kidney lysates. This may suggest that BNP does not directly suppress cAMP. Since Src inhibition has demonstrated reduced cystogenesis independent from renal cAMP levels,[30] it is plausible

that BNP targets effectors downstream of the cAMP pathway, such as suppression of the Ras/B-Raf/ERK pathway through PKG-II-mediated ErbB2/Her2 suppression.[31, 32] Since increased intracellular Ca^{2+} restores inhibitory effects of cAMP against cell proliferation and ERK phosphorylation in primary cultured PKD cells,[29] it is also possible that the 'switching' of cAMP-responsive characteristics, regulated by intracellular Ca^{2+} concentration, may also play an inhibitory role, as BNP treatment restores intracellular Ca^{2+} levels in cystic epithelia cells. Further studies will elucidate a potential anti-proliferative and ERK inhibitory roles of cAMP in BNP treatment.

Roles of the cGMP pathways in PKD

cGMP is synthesized by natriuretic peptide-activated particulate guanylyl cyclases (pGCs) or by NO-activated soluble guanylyl cyclase (sGC).[33] Although recent studies have implicated crosstalk between cAMP and cGMP pathways in PKD, through cAMP- and/or cGMP-degrading phosphodiesterases (PDEs),[34] the role of cGMP signaling on the development, or progression, of PKD is poorly understood. cGMP levels are increased in cystic kidneys of PKD animals.[11] *In vitro* studies have demonstrated that cGMP supplementation modestly increases *in vitro* MDCK cyst expansion.[11] In contrast, 8-Br-cGMP treatment does not affect the proliferation of primary human PKD cyst-derived cells.[12] Our data demonstrates cGMP induction through the BNP/GC-A axis reduces cystogenesis in the PCK rat. This discrepancy may be due to compartmentalized and unique GCs, which then stimulate distinct effectors.[35] For instance, GC-A-induced cGMP is degraded primarily by PDE2 while GC-B-induced cGMP is degraded by PED3.[36, 37] PDE1 is largely responsible for renal cGMP PDE activity,[11] suggesting that renal cGMP is produced through sGC activation and degraded by PDE1. Thus, GC-A-mediated cGMP may activate effectors, distinct from those activated by the NO/sGC axis in cystic kidneys. Another possibility is that cGMP elevation is compensatory. Multiple studies demonstrate marked renoprotective effects of sustained activation of GC-A and GC-B by BNP and CNP, respectively.[9, 10, 38] Moreover, the endothelial NO synthase Glu298Asp mutation responsible for impaired NO production[39] is associated with a 5-year lower mean age at ESRD in ADPKD patients,[39] supporting the renoprotective effects of sGC-induced cGMP in PKD. Thus, further studies are warranted to define specific effectors and chronic GC-A activation in PKD.

BNP antiproliferative effects and increased $[Ca^{2+}]_i$ in renal and hepatic epithelial cells

In cardiomyocytes, cGMP activates PKG-I to reduce cytoplasmic $[Ca^{2+}]_i$ through inhibition of Ca^{2+} influx by L-type Ca2+ channels, leading to relaxation and inhibition of cardiac hypertrophy.[40, 41] Here, BNP increased $[Ca^{2+}]_I$ in renal and hepatic epithelial cells, mediated partly through IP_3R. This discrepancy may be due to differentially expressed PKG isoforms. PKG-II is ubiquitous throughout the nephron, with the highest levels in juxtaglomerular cells and tubules.[42] Activation of PKG-II through the GC-A/cGMP axis has been shown to stimulate Ca^{2+} reabsorption.[43] PKG-II activation can also phosphorylate IP_3R, increasing cytosolic $[Ca^{2+}]$ in hippocampal neurons and hepatocytes.[44, 45] We postulate that BNP increases $[Ca^{2+}]_i$ levels in renal epithelium through activation of PKG-II.

Liver-protective effects

Though BNP reduced cysts with trends of reduced connective tissue, *Col1a1* transcripts and hepatic collagen content were not reduced by AAV9-BNP. This suggests BNP treatment enhanced matrix degradation instead of inhibiting activation of hepatic stellate cells and/or portal fibroblasts. Conversely, we found suppression of Desmin-positive, but αSMA-negative, hepatic stellate-like cell expansion by BNP treatment. At 4 months, we saw induction of Desmin- and αSMA-double positive myofibroblasts-like cells in control rats, which appeared to be reduced by BNP treatment. Similarly, BNP-transgenic mice are resistant to hepatic damage, liver fibrosis, and suppressed stellate cell activation and Tgfβ induction.[46] Further studies are warranted to define underlying collagen independent BNP anti-fibrotic effects in the liver.

pERK levels in vivo

In concert with our in vitro study, we found reduced pERK levels in the AAV-BNP-treated liver (Supplementary Fig. S11). However, we found no notable changes in pERK levels in BNP-treated kidneys. It is possible that BNP-mediated suppression of pERK in cystic cells in vivo is not strong and masked by abundant pERK in other types of renal cells.

AAV vector-mediated gene therapy for renal diseases

Previously, we demonstrated no notable toxicity 9 months post AAV9 administration in a hypertensive rat model.[15] In PCK, blood chemistry revealed no detectable difference in low- or HD AAV9-BNP treatments 3 months post administration (Sup. Fig. S1 and S7B). We also found no notable toxicity, nor beneficial effects, in PCK treated with luciferase-expressing AAV9 (Sup. Fig. S12). AAV9 vectors are established for their robust transduction of variety cell types; heart, liver, kidney, and endothelial cells in adult animals, while neonatal administration of AAV9 leads to near whole-body transduction.[47–50] Consistent with previous reports, AAV9 in our PCK, exhibited widespread transgene expression in the heart, liver, and kidneys. However, BNP renal transgene transcripts were still approximately 100-fold less than cardiac upon neonatal AAV9 administration. Kidney targeted optimization of AAV will further improve BNP gene therapy for PKD.

Sample numbers

We maintained multiple PCK breeding pairs, with a study design allowing for sufficient numbers for treated and control groups. However, an unexpectedly high incidence of maternal cannibalism, associated with neonatal AAV transduction, limited the study. Additionally, we observed significant gender-bias in litters, with reduced numbers of male PCK pups, possibly due to increased embryonic lethality in males. Thus, our data set focuses on females. All animal manipulations were carried out for both treatment groups with preserved time intervals. For echocardiography, blood pressure, and metabolic tests, all animals from each treatment group were assayed and included in the figure, baring animals that didn’t produce analyzable data. For assays on stored biological material, we used samples from treated and control rats from the same litters to reduce possible inter-litter variations.

Conclusions

Our study demonstrates long-term therapeutic, and multifaceted effects of BNP in a clinically relevant PKD model, the PCK rat, on hepatorenal cystogenesis.[13, 14] While the role of cAMP signaling in PKD has received much attention,[51] our study suggests the influence of cGMP signaling on the progression of PKD *in vivo*. Together with cardioprotective effects, sustained BNP and/or GC-A-stimulating strategies may present a novel avenue for preventing PKD progression and associated complications.

METHODS

Animals, Plasmids, Vectors, Data, and Statistical Analysis are detailed in the Supplemental Text.

Supplementary Material

Refer to Web version on PubMed Central for supplementary material.

Acknowledgments

We thank Mayo's Translational Polycystic Kidney Disease Center, Jim Tarara, Shawna Cooper, Vlad Gainullin, Katharina Hopp, and Maria Lorenzo Pisarello for their time, reagents, and invaluable advice.

Funding source(s): National Institute of Health R01 HL098502 (to AC and YI), Mayo PKD Center Pilot Study Award (to AC and YI, parent grant NIDDK P30DK90728, PI: VET), Mayo Foundation (to Y.I.), NIDDK DK024031 (to NFL), and Mayo Graduate School (to SJH)

References

1. Chapman AB, Devuyst O, Eckardt KU, et al. Autosomal-dominant polycystic kidney disease (ADPKD): executive summary from a Kidney Disease: Improving Global Outcomes (KDIGO) Controversies Conference. Kidney Int. 2015; 88:17–27. [PubMed: 25786098]
2. Ong AC, Devuyst O, Knebelmann B, et al. Autosomal dominant polycystic kidney disease: the changing face of clinical management. Lancet. 2015; 385:1993–2002. [PubMed: 26090645]
3. Adeva M, El-Youssef M, Rossetti S, et al. Clinical and molecular characterization defines a broadened spectrum of autosomal recessive polycystic kidney disease (ARPKD). Medicine (Baltimore). 2006; 85:1–21. [PubMed: 16523049]
4. Cowley BD Jr. Calcium, cyclic AMP, and MAP kinases: dysregulation in polycystic kidney disease. Kidney Int. 2008; 73:251–253. [PubMed: 18195694]
5. Fedeles SV, Gallagher AR, Somlo S. Polycystin-1: a master regulator of intersecting cystic pathways. Trends Mol Med. 2014; 20:251–260. [PubMed: 24491980]
6. Zellner C, Protter AA, Ko E, et al. Coronary vasodilator effects of BNP: mechanisms of action in coronary conductance and resistance arteries. Am J Physiol. 1999; 276:H1049–1057. [PubMed: 10070091]
7. Fujisaki H, Ito H, Hirata Y, et al. Natriuretic peptides inhibit angiotensin II-induced proliferation of rat cardiac fibroblasts by blocking endothelin-1 gene expression. J Clin Invest. 1995; 96:1059–1065. [PubMed: 7635942]
8. Holditch SJ, Schreiber CA, Nini R, et al. B-Type Natriuretic Peptide Deletion Leads to Progressive Hypertension, Associated Organ Damage, and Reduced Survival: Novel Model for Human Hypertension. Hypertension. 2015; 66:199–210. [PubMed: 26063669]
9. Suganami T, Mukoyama M, Sugawara A, et al. Overexpression of brain natriuretic peptide in mice ameliorates immune-mediated renal injury. J Am Soc Nephrol. 2001; 12:2652–2663. [PubMed: 11729234]

10. Makino H, Mukoyama M, Mori K, et al. Transgenic overexpression of brain natriuretic peptide prevents the progression of diabetic nephropathy in mice. Diabetologia. 2006; 49:2514–2524. [PubMed: 16917760]
11. Wang X, Ward CJ, Harris PC, et al. Cyclic nucleotide signaling in polycystic kidney disease. Kidney Int. 2010; 77:129–140. [PubMed: 19924104]
12. Hanaoka K, Guggino WB. cAMP regulates cell proliferation and cyst formation in autosomal polycystic kidney disease cells. J Am Soc Nephrol. 2000; 11:1179–1187. [PubMed: 10864573]
13. Lager DJ, Qian Q, Bengal RJ, et al. The pck rat: a new model that resembles human autosomal dominant polycystic kidney and liver disease. Kidney Int. 2001; 59:126–136. [PubMed: 11135065]
14. Ward CJ, Hogan MC, Rossetti S, et al. The gene mutated in autosomal recessive polycystic kidney disease encodes a large, receptor-like protein. Nat Genet. 2002; 30:259–269. [PubMed: 11919560]
15. Cataliotti A, Tonne JM, Bellavia D, et al. Long-term cardiac pro-B-type natriuretic peptide gene delivery prevents the development of hypertensive heart disease in spontaneously hypertensive rats. Circulation. 2011; 123:1297–1305. [PubMed: 21403100]
16. Matsukawa N, Grzesik WJ, Takahashi N, et al. The natriuretic peptide clearance receptor locally modulates the physiological effects of the natriuretic peptide system. Proc Natl Acad Sci U S A. 1999; 96:7403–7408. [PubMed: 10377427]
17. Riphagen IJ, Boertien WE, Alkhalaf A, et al. Copeptin, a surrogate marker for arginine vasopressin, is associated with cardiovascular and all-cause mortality in patients with type 2 diabetes (ZODIAC-31). Diabetes Care. 2013; 36:3201–3207. [PubMed: 23757433]
18. Lee EJ, Song SA, Mun HW, et al. Blockade of interleukin-8 receptor signalling inhibits cyst development in vitro, via suppression of cell proliferation in autosomal polycystic kidney disease. Nephrology (Carlton). 2014; 19:471–478. [PubMed: 24724588]
19. Wilson SJ, Amsler K, Hyink DP, et al. Inhibition of HER-2(neu/ErbB2) restores normal function and structure to polycystic kidney disease (PKD) epithelia. Biochim Biophys Acta. 2006; 1762:647–655. [PubMed: 16797938]
20. Peters DJ, Breuning MH. Autosomal dominant polycystic kidney disease: modification of disease progression. Lancet. 2001; 358:1439–1444. [PubMed: 11705510]
21. Sonoyama T, Tamura N, Miyashita K, et al. Inhibition of hepatic damage and liver fibrosis by brain natriuretic peptide. FEBS Lett. 2009; 583:2067–2070. [PubMed: 19463821]
22. Huntley BK, Ichiki T, Sangaralingham SJ, et al. B-type natriuretic peptide and extracellular matrix protein interactions in human cardiac fibroblasts. J Cell Physiol. 2010; 225:251–255. [PubMed: 20506274]
23. Ichiki T, Schirger JA, Huntley BK, et al. Cardiac fibrosis in end-stage human heart failure and the cardiac natriuretic peptide guanylyl cyclase system: regulation and therapeutic implications. J Mol Cell Cardiol. 2014; 75:199–205. [PubMed: 25117468]
24. Tamura N, Ogawa Y, Chusho H, et al. Cardiac fibrosis in mice lacking brain natriuretic peptide. Proceedings of the National Academy of Sciences of the United States of America. 2000; 97:4239–4244. [PubMed: 10737768]
25. Hassane S, Leonhard WN, van der Wal A, et al. Elevated TGFbeta-Smad signalling in experimental Pkd1 models and human patients with polycystic kidney disease. J Pathol. 2010; 222:21–31. [PubMed: 20549648]
26. Liu D, Wang CJ, Judge DP, et al. A Pkd1-Fbn1 genetic interaction implicates TGF-beta signaling in the pathogenesis of vascular complications in autosomal dominant polycystic kidney disease. J Am Soc Nephrol. 2014; 25:81–91. [PubMed: 24071006]
27. Leonhard WN, Kunnen SJ, Plugge AJ, et al. Inhibition of Activin Signaling Slows Progression of Polycystic Kidney Disease. J Am Soc Nephrol. 2016
28. Yamaguchi T, Wallace DP, Magenheimer BS, et al. Calcium restriction allows cAMP activation of the B-Raf/ERK pathway, switching cells to a cAMP-dependent growth-stimulated phenotype. The Journal of biological chemistry. 2004; 279:40419–40430. [PubMed: 15263001]
29. Yamaguchi T, Hempson SJ, Reif GA, et al. Calcium restores a normal proliferation phenotype in human polycystic kidney disease epithelial cells. J Am Soc Nephrol. 2006; 17:178–187. [PubMed: 16319189]

30. Sweeney WE Jr, von Vigier RO, Frost P, et al. Src inhibition ameliorates polycystic kidney disease. J Am Soc Nephrol. 2008; 19:1331–1341. [PubMed: 18385429]
31. Chen WS, Leung CM, Pan HW, et al. Silencing of miR-1-1 and miR-133a-2 cluster expression by DNA hypermethylation in colorectal cancer. Oncol Rep. 2012; 28:1069–1076. [PubMed: 22766685]
32. Cao ZH, Tao Y, Sang JR, et al. Type II, but not type I, cGMP-dependent protein kinase reverses bFGF-induced proliferation and migration of U251 human glioma cells. Mol Med Rep. 2013; 7:1229–1234. [PubMed: 23404188]
33. Liu Y, Ruoho AE, Rao VD, et al. Catalytic mechanism of the adenylyl and guanylyl cyclases: modeling and mutational analysis. Proceedings of the National Academy of Sciences of the United States of America. 1997; 94:13414–13419. [PubMed: 9391039]
34. Pinto CS, Raman A, Reif GA, et al. Phosphodiesterase Isoform Regulation of Cell Proliferation and Fluid Secretion in Autosomal Dominant Polycystic Kidney Disease. J Am Soc Nephrol. 2016; 27:1124–1134. [PubMed: 26289612]
35. Moltzau LR, Aronsen JM, Meier S, et al. Different compartmentation of responses to brain natriuretic peptide and C-type natriuretic peptide in failing rat ventricle. J Pharmacol Exp Ther. 2014; 350:681–690. [PubMed: 25022512]
36. Cai YL, Sun Q, Huang X, et al. cGMP-PDE3-cAMP signal pathway involved in the inhibitory effect of CNP on gastric motility in rat. Regul Pept. 2013; 180:43–49. [PubMed: 23186653]
37. Wen JF, Quan HX, Zhou GH, et al. Altered role of C-type natriuretic peptide-activated pGC-cGMP-PDE3-cAMP signaling in hyperthyroid beating rabbit atria. Regul Pept. 2007; 142:123–130. [PubMed: 17531330]
38. Kimura T, Nojiri T, Hosoda H, et al. Protective effects of C-type natriuretic peptide on cisplatin-induced nephrotoxicity in mice. Cancer Chemother Pharmacol. 2015; 75:1057–1063. [PubMed: 25814217]
39. Noiri E, Satoh H, Taguchi J, et al. Association of eNOS Glu298Asp polymorphism with end-stage renal disease. Hypertension. 2002; 40:535–540. [PubMed: 12364359]
40. Mery PF, Lohmann SM, Walter U, et al. Ca2+ current is regulated by cyclic GMP-dependent protein kinase in mammalian cardiac myocytes. Proc Natl Acad Sci U S A. 1991; 88:1197–1201. [PubMed: 1705030]
41. Fiedler B, Lohmann SM, Smolenski A, et al. Inhibition of calcineurin-NFAT hypertrophy signaling by cGMP-dependent protein kinase type I in cardiac myocytes. Proc Natl Acad Sci U S A. 2002; 99:11363–11368. [PubMed: 12177418]
42. Gambaryan S, Hausler C, Markert T, et al. Expression of type II cGMP-dependent protein kinase in rat kidney is regulated by dehydration and correlated with renin gene expression. J Clin Invest. 1996; 98:662–670. [PubMed: 8698857]
43. Hoenderop JG, Vaandrager AB, Dijkink L, et al. Atrial natriuretic peptide-stimulated Ca2+ reabsorption in rabbit kidney requires membrane-targeted, cGMP-dependent protein kinase type II. Proceedings of the National Academy of Sciences of the United States of America. 1999; 96:6084–6089. [PubMed: 10339545]
44. Bredt DS, Snyder SH. Nitric oxide, a novel neuronal messenger. Neuron. 1992; 8:3–11. [PubMed: 1370373]
45. Guihard G, Combettes L, Capiod T. 3′:5′-cyclic guanosine monophosphate (cGMP) potentiates the inositol 1,4,5-trisphosphate-evoked Ca2+ release in guinea-pig hepatocytes. Biochem J. 1996; 318(Pt 3):849–855. [PubMed: 8836128]
46. Sonoyama T, Tamura N, Miyashita K, et al. Inhibition of hepatic damage and liver fibrosis by brain natriuretic peptide. FEBS Lett. 2009; 583:2067–2070. [PubMed: 19463821]
47. Ghosh A, Yue Y, Long C, et al. Efficient whole-body transduction with trans-splicing adeno-associated viral vectors. Mol Ther. 2007; 15:750–755. [PubMed: 17264855]
48. Yue Y, Ghosh A, Long C, et al. A single intravenous injection of adeno-associated virus serotype-9 leads to whole body skeletal muscle transduction in dogs. Mol Ther. 2008; 16:1944–1952. [PubMed: 18827804]

49. Saunders NR, Joakim Ek C, Dziegielewska KM. The neonatal blood-brain barrier is functionally effective, and immaturity does not explain differential targeting of AAV9. Nat Biotechnol. 2009; 27:804–805. author reply 805. [PubMed: 19741632]

50. Gadalla KK, Bailey ME, Spike RC, et al. Improved survival and reduced phenotypic severity following AAV9/MECP2 gene transfer to neonatal and juvenile male Mecp2 knockout mice. Mol Ther. 2013; 21:18–30. [PubMed: 23011033]

51. Torres VE, Harris PC. Strategies targeting cAMP signaling in the treatment of polycystic kidney disease. J Am Soc Nephrol. 2014; 25:18–32. [PubMed: 24335972]

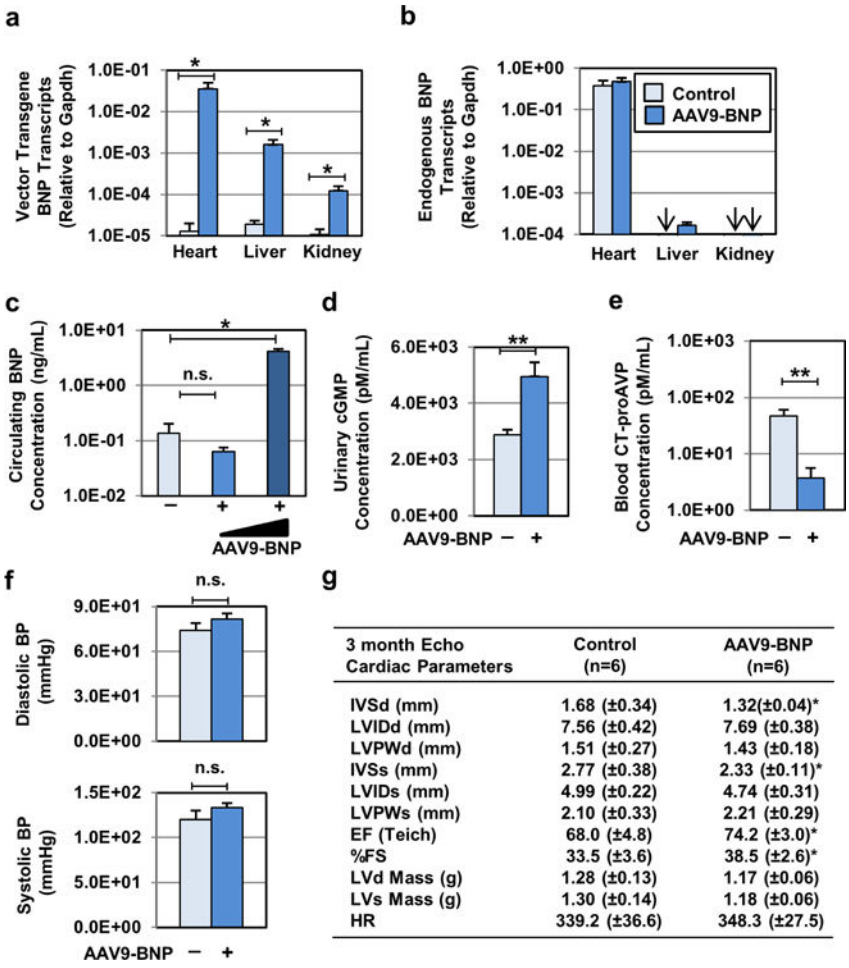

g

3 month Echo Cardiac Parameters	Control (n=6)	AAV9-BNP (n=6)
IVSd (mm)	1.68 (±0.34)	1.32(±0.04)*
LVIDd (mm)	7.56 (±0.42)	7.69 (±0.38)
LVPWd (mm)	1.51 (±0.27)	1.43 (±0.18)
IVSs (mm)	2.77 (±0.38)	2.33 (±0.11)*
LVIDs (mm)	4.99 (±0.22)	4.74 (±0.31)
LVPWs (mm)	2.10 (±0.33)	2.21 (±0.29)
EF (Teich)	68.0 (±4.8)	74.2 (±3.0)*
%FS	33.5 (±3.6)	38.5 (±2.6)*
LVd Mass (g)	1.28 (±0.13)	1.17 (±0.06)
LVs Mass (g)	1.30 (±0.14)	1.18 (±0.06)
HR	339.2 (±36.6)	348.3 (±27.5)

Fig. 1. Characterization of single intraperitoneal AAV9 vector administration in neonatal female PCK rats

(a) Biodistribution of AAV9 vector upon neonatal AAV9 vector administration was monitored. Codon-optimized vector transgene BNP and (b) endogenous BNP transcript levels in the heart, kidney, and liver samples were determined by RT-PCR, followed by normalization to Gapdh transcript levels. Control (n=8) and AAV9-BNP vector-treated (n=6, 1.0×10^{13} vg/kg) PCK rats were used. Arrows indicate where transcripts assayed were below detection. (c) Circulating levels of BNP from littermate control PCK (n=6), AAV9-BNP (n=9, 1.0×10^{13} vg/kg) and High-Dose AAV9-BNP (n=5, 1.0×10^{14} vg/kg) were determined by rat BNP45 ELISA. (d) Urinary excreted cyclic GMP (cGMP) and (e) plasma levels of CT-proAVP from control (n=10) and AAV9-BNP (n=10, 1.0×10^{13} vg/kg) were determined. (f) Noninvasive diastolic and systolic blood pressure measurements were determined in AAV9-BNP-treated (n=15, 1.0×10^{13} vg/kg) and control littermate PCK rats (n=10). Both groups remained normotensive 3 months post treatment. (g) Echocardiographic assessment (Echo) of cardiac structure and function was performed in PCK (n=7) and AAV9-BNP-treated (n=10, 1.0×10^{13} vg/kg) groups. Improved cardiac function and reduced cardiac mass were associated with AAV9-BNP vector administration. Intraventricular septum, diastole (IVSd), Left ventricular internal diameter, diastole (LVIDd), Left ventricular posterior wall, diastole (LVPWd), Intraventricular septum, systole (IVSs), Left ventricular internal

diameter, systole (LVIDs), Left ventricular posterior wall, systole (LVPWs), Ejection Fraction (EFteich), Percent fractional shortening (%FS), Left ventricular Mass, diastole (LVd Mass), Left ventricular mass, Systole (LVs Mass). *$P < 0.05$ and **$P < 0.01$, vs. PCK by t test. Data represent the mean ± SEM.

a

	Urinalysis	Control (n=8)	AAV9-BNP (n=7)	Sprague Dawley (no PKD control, n=6)
Urine Metabolites	Urine (unadjusted)			
	Sodium (mM/L)	85 ± 20	130 ± 39*	134 ± 23
	Potassium (mM/L)	282 ± 75	396 ± 41*	356 ± 48
	Creatinine (mg/dL)	66 ± 22	88 ± 22	100 ± 18†
	Protein(mg/dL)	488 ± 267	268 ± 186*	ND
	Urine (mL/24hr)	13.3 ± 1.8	7.6 ± 2.3*	12.7 ± 1.4!
	Sodium (mM/24hr)	1.1 ± 0.1	1.4 ± 0.2	1.7 ± 0.2†
	Potassium (mM/24h)	3.5 ± 0.2	3.0 ± 0.3	4.5 ± 0.4
	Creatinine (mg/24h)	8.1 ± 0.6	9.2 ± 1.1	12.2 ± 0.7†
	Protein (mg/24h)	57.1 ± 19.5	36.0 ± 11.5	ND

b

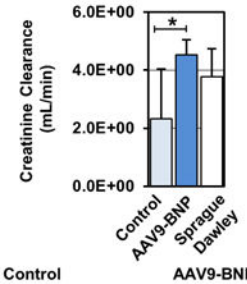

c

	Control	AAV9-BNP	Sprague Dawley
BW (g)	269.4 ± 15.7	289.5 ± 19.0	262.6 ± 10.9!!
LKW/BW (mg/g)	6.9 ± 0.9	6.1 ± 0.9*	3.4 ± 0.3†††!!!
RKW/BW (mg/g)	7.5 ± 1.1	6.5 ± 0.9*	3.7 ± 0.2†††!!!
TKW/BW (mg/g)	14.5 ± 2.0	12.6 ± 1.7*	7.0 ± 0.5†††!!!

d

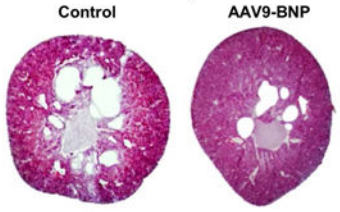

e

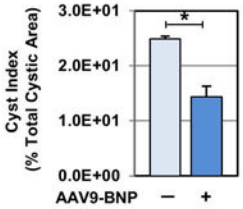

f

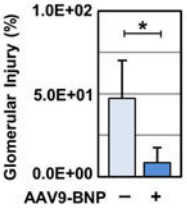

g

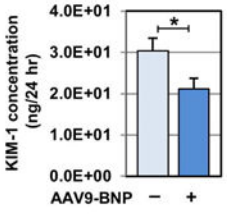

h

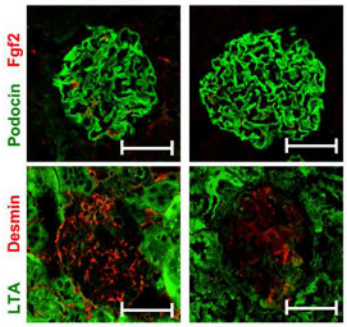

i

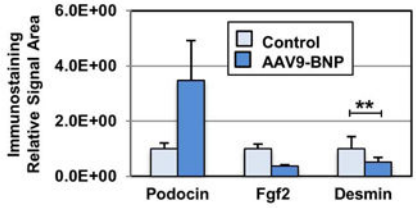

j

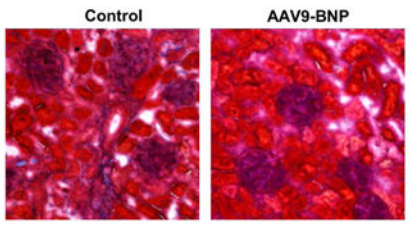

k

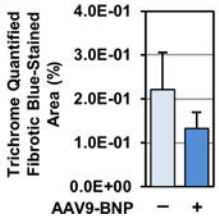

l

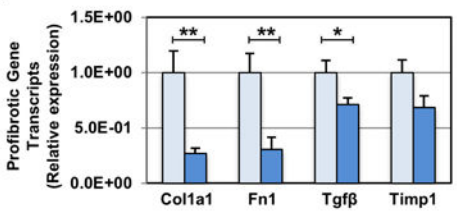

m

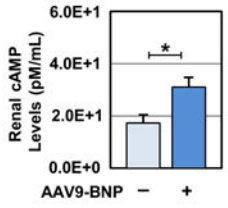

Fig. 2. BNP overexpression reduces kidney size, renal cyst growth, interstitial fibrosis and glomerular injury in female PCK rats

(a) Urine volume and urinary test parameters were determined in AAV9-BNP-treated, control PCK and SD rats. (b) Estimated creatinine clearance was determined by blood and urinary creatinine concentrations, and compared among the AAV9-BNP-treated, control PCK and SD rat groups. Control (n=10), AAV9-BNP (n=10, 1.0×10^{13} vg/kg) treated PCK and SD (n=6) rats were used (a–c). (c) Total body weight (BW) and left, right and total kidney weight to BW ratios at 3 months post injection are shown. (d) Representative Hematoxylin and Eosin (H&E)-staining images of renal sections from AAV9-BNP-treated

and untreated PCK rats are shown. (e) Renal cystic index was determined using the H&E-staining images of control (n=7) and AAV9-BNP vector-treated (n=7, 1.0×10^{13} vg/kg) PCK rats. (f) Percent glomerular injury was quantified using H&E staining images of kidney sections of control and treated PCK rats (n=5 each, 4 images/animal). (g) Urinary excretion of tubular epithelial injury marker Kidney Injury Molecule-1 (KIM-1) was determined by ELISA. (h) Representative images of immunofluorescent microscopy of the glomeruli of control and AAV9-BNP vector-treated PCK rats are shown. Anti-basic fibroblast growth factor 2 (Fgf2, Red) and anti-podocin (Blue) antibodies (upper panels), and anti-Desmin (Red) and anti-lotus tetragonolobus (LTA, Green) antibodies were used. Nuclei were counterstained with DAPI (White). (i) Relative staining of immunofluorescent images of control and AAV9-BNP-treated PCK rats were determined (n=5 each, 4 images/animal). (j) Representative images (20×, zoomed in 25% in Adobe Photoshop CC 2015) of trichrome stained renal sections from PCK treated and control rats. (k) Interstitial fibrosis quantified from trichrome stained kidney sections (n=5 treated, n=4 PCK control). (l) Levels of Collagen type 1a1 (Col1a1), Fibronectin-1 (Fn1), Transforming growth factor-beta (Tgfβ) and Tissue inhibitor metalloprotease-1 (Timp1) transcripts were analyzed by RT-PCR. Relative transcript levels were determined using Gapdh transcript levels, and compared to littermate controls. Total kidney RNA samples from control (n=7) and AAV9-BNP vector-treated (n=7, 1.0×10^{13} vg/kg) PCK rats were used. (m) Renal cyclic AMP (cAMP) levels in control and AAV9-BNP vector-treated and PCK rats were determined (n=10 each). (l) $*P < 0.05$, $**P < 0.01$, and $***P < 0.001$ (AAV9-BNP treated vs. PCK controls, by *t* test). †$P<0.05$, ††$P<0.01$, and †††$P<0.001$ (PCK controls vs. SD, by *t* test). !$P<0.05$, !!$P<0.01$, !!!$P<0.001$ (AAV9-BNP treated vs. SD by *t* test). Data represent the mean ± SEM.

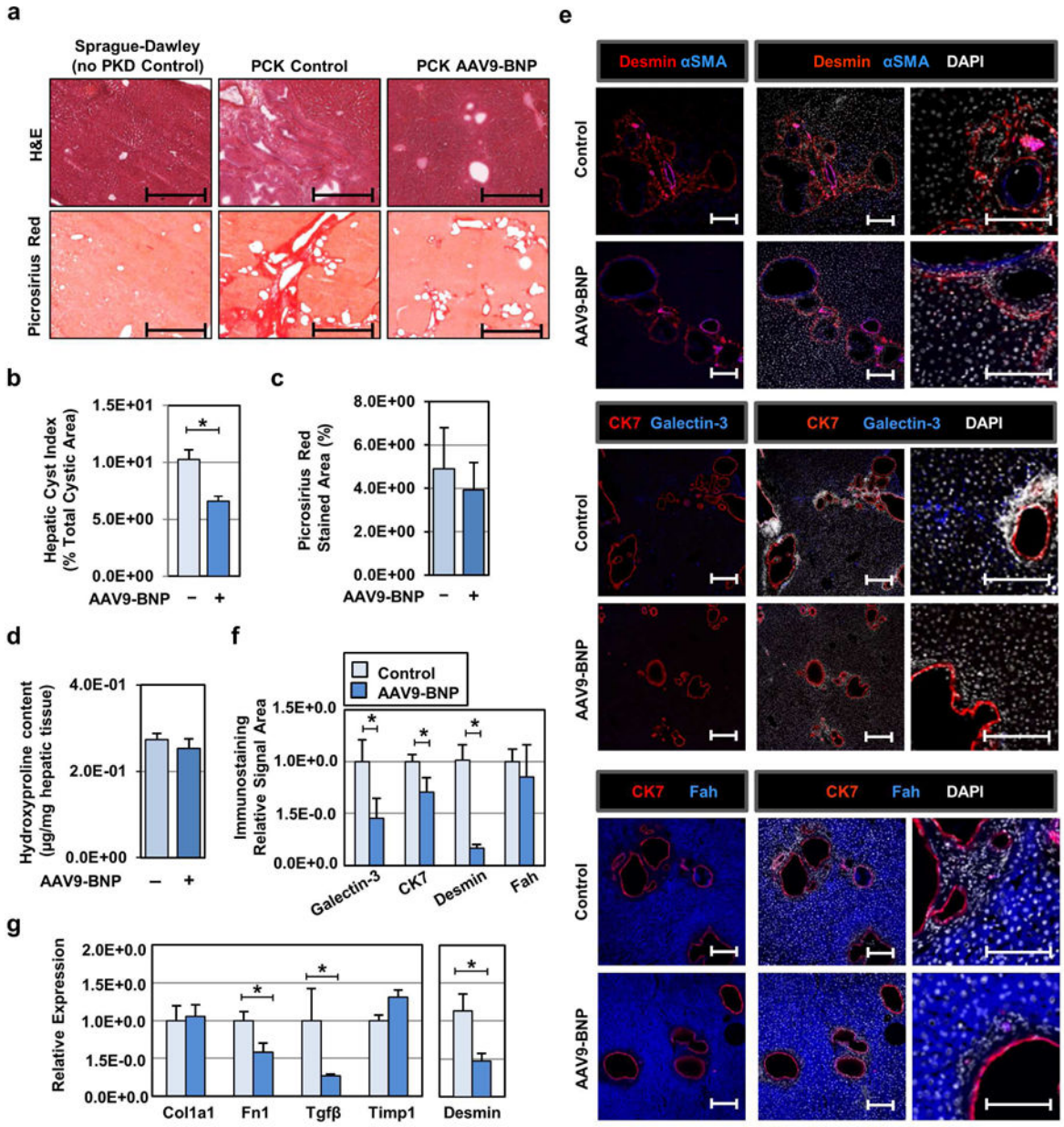

Fig. 3. Sustained BNP treatment reduces cystic lesions, fibrosis and profibrotic gene expression in the liver of female PCK rats

(a) Representative hematoxylin and eosin (H&E) staining images of hepatic sections 3 months' post AAV9-BNP vector administration (top panels), and representative picosirius red staining images are shown (bottom panels). Age-matched livers from non PKD control (Sprague-Dawley rat), control PCK and AAV9-BNP vector-treated PCK rats were used. Scale bars; 1 mm. (b) Hepatic cystic index was determined using the H&E-staining images of control (n=7) and AAV9-BNP vector-treated (n=7, 1.0×10^{13} vg/kg) PCK rats. (c) We determined fibrotic areas as measured from picosirius red stained liver sections (n=5 treated, n=4 PCK controls). (d) Hepatic hydroxyproline levels in PCK control (n=4) and AAV9-BNP treated (n=6) PCK rats were determined to estimate collagen content. (e) Representative images of immunofluorescent staining of hepatic sections are shown. Anti-Desmin(red) and

anti-alpha-Smooth Muscle Actin (blue) antibodies (top), anti-CK7 (red) and anti-Galectin-3 (green) antibodies (middle) and anti-fumarylacetoacetate hydrolase (Fah, blue) and anti-CK7 (red) antibodies (bottom) were used for immunostaining. Nuclei were counterstained by DAPI (white). Scale bars; 1.0 μm. (f) Individual immunofluorescent signal areas in (e) were quantified and shown as mean fluorescent signal areas, relative to control PCK littermates. Immunofluorescent images of control (n=4) and AAV9-BNP vector-treated (n=7, 1.0×10^{13} vg/kg) PCK rats were used. (g) Levels of Collagen type 1a1 (Col1a1), Fibronectin-1 (Fn1), Transforming growth factor-β (Tgfβ), Tissue inhibitor metalloprotease-1 (Timp1) and Desmin transcripts were determined by RT-PCR, corrected for Gapdh transcripts, and presented relative to those found in control littermates. Control (n=8) and AAV9-BNP vector-treated (n=6, 1.0×10^{13} vg/kg) PCK rats were used. $*P < 0.05$. (vs. PCK controls, by *t* test) Data represent the mean ± SEM.

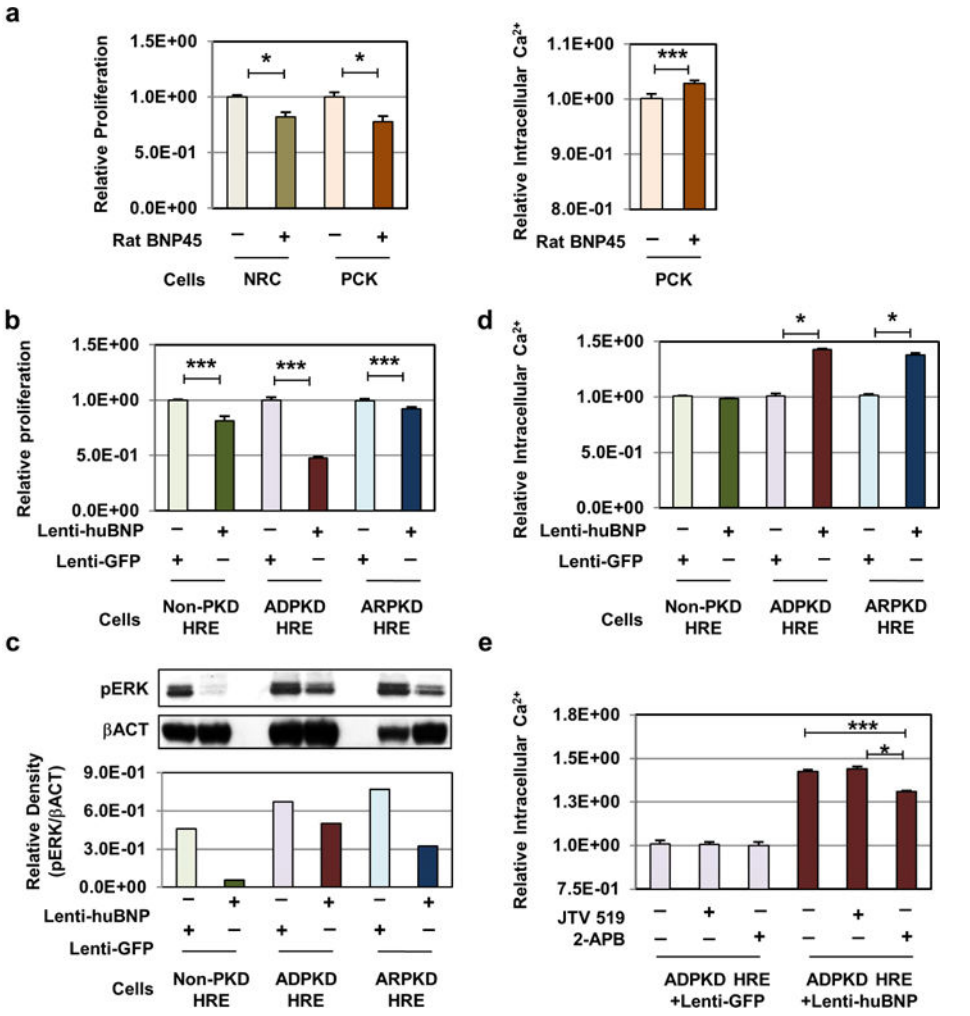

Fig. 4. BNP treatment reduces proliferation and increases intracellular calcium in primary PKD epithelial cells

(a) *In vitro* proliferation studies of normal (NRC) and cystic (PCK) rat cholangiocytes derived from Sprague Dawley and PCK rats. Cells were treated with normal growth media (light grey/pink bars) or 270 nmol rat-BNP peptide-spiked media (green/orange bars), and assayed for relative proliferation 72 hours post plating (left panel). Intracellular calcium levels were determined in PCK rat-derived cholangiocytes cultured in media supplemented with (orange bar) and without (pink bar) 270nmol rat-BNP peptide, assayed by Fura-2 AM calcium quantification (right panel). Data represents a mean of 6 individual assays, each with 24 replicates ± SEM. (b) Patient-derived noncystic, normal human renal epithelial cells (Non-PKD HRE), and ADPKD and ARPKD cystic human renal epithelial cells (ADPKD HRE, ARPKD HRE) were transduced with lentiviral vectors expressing control Green Fluorescent Protein (Lenti-GFP), or codon-optimized human BNP (Lenti-huBNP). GFP- and human BNP-expressing HRE cells were assayed for relative proliferative ability, 48–72 hours post-plating. Proliferation rates are expressed as relative to Lenti-GFP vector-treated control cells. Data represents a minimum mean of 3 individual assays, with a minimum of 20 replicates ± SEM. *$P < 0.05$, **$P < 0.01$, and ***$P < 0.001$, vs. Lenti-GFP by *t* test. (c) Levels of phosphorylated-extracellular-signal-regulated-kinase (PERK) protein were

determined by Western blotting using non-cystic and PKD-derived cystic HRE cells transduced with Lenti-GFP, or Lenti-huBNP. (d) Intracellular calcium levels were determined by Fura-2 AM calcium quantification assay. Data represents a mean of 6 individual assays, each with 24 replicates ± SEM. (e) Intracellular calcium levels were quantified in the presence of ER-calcium channel inhibitors, 2-ABP (100 μM) or JTV 519 (1μm), or vehicle. ADPKD HRE cells transduced with Lenti-GFP or Lenti-huBNP were used for the assay. Data points represent the mean of a minimum of 24 replicates ± SEM. $*P < 0.05$ and $***P < 0.001$, vs. Lenti-GFP by *t* test.